NeuroImage **11,** 58–65 (2000)
doi:10.1006/nimg.1999.0517, available online at http://www.idealibrary.com on IDEAL®

RAPID COMMUNICATION

# Real-Time Monitoring of Eye Movements Using Infrared Video-oculography during Functional Magnetic Resonance Imaging of the Frontal Eye Fields

Darren R. Gitelman,*,†,‡ Todd B. Parrish,† Kevin S. LaBar,* and M.-Marsel Mesulam*

**Department of Neurology and †Department of Radiology, Northwestern Cognitive Brain Mapping Group, The Cognitive Neurology and Alzheimer's Disease Center, Northwestern University Medical School, and ‡Lakeside Division, Chicago V.A. Healthcare System, Chicago, Illinois 60611*

Received July 6, 1999

**Monitoring eye movements is a critical aspect of experimental design for studies of spatial attention and visual perception. However, obtaining online eye-movement recordings has been technologically difficult during functional magnetic resonance (MR) imaging studies. Previous approaches to monitoring eye movements either have distorted the MR images or have shown MR-related interference in the recordings. We report a technique using long-range infrared video-oculography to record eye movements without causing artifacts in the MR images. Analysis of the MR signal from a phantom obtained with the eye-movement equipment turned on or off confirmed the absence of significant additional noise in the MR time series. Eye movements of three subjects were monitored while they performed tasks of covert and overt shifts of spatial attention. Activation of the frontal eye fields during the covert task was seen even when the eye-movement recordings demonstrated no significant difference in saccadic eye movements between the baseline and the active conditions.** © 2000 Academic Press

## INTRODUCTION

The control of eye movements is a critical aspect of experimental design in functional imaging studies of visual perception and visuospatial attention (Corbetta *et al.,* 1993; Gitelman *et al.,* 1999; Kim *et al.,* 1999; Nobre *et al.,* 1997). Monitoring eye movements during such studies is therefore necessary in order to determine whether subjects have been able to perform the task correctly. The failure to obtain this information makes it difficult to specify whether regional activations, such as those in the frontal eye fields, can be attributed to the cognitive task or to improper eye movements.

To date, all reported methods of monitoring eye movements during functional magnetic resonance imaging (fMRI) have suffered from a number of limitations (Brandt *et al.,* 1997; Culham *et al.,* 1998; Felblinger *et al.,* 1996; Greenlee *et al.,* 1999). For example, Culham and colleagues (1998) monitored eye movements using infrared light-emitting diodes and photodetectors mounted on goggles (Ober2; Permobil Medtech AB, Sweden). This system produced interpretable eye movement recordings, but not without "substantial artifacts in the eye movement traces" during MR acquisition (Culham *et al.,* 1998). Furthermore, the device's circuit board caused distortions in frontal lobe MR signals (R. Savoy, MGH-NMR Center, personal communication, and S. Aisenberg, Permobil Medtech AB, personal communication).

The use of electro-oculographic (EOG) methods during echo planar imaging (EPI) was first reported by Felblinger *et al.* (1996). They designed an EOG amplifier and fiber-optic transmission system which attempted to minimize the interactions between the fMRI and the EOG signals. Although the EOG signal was not affected by the gradient magnetic field switching associated with EPI, the system had a low overall resolution—on the order of 5° of visual angle (C. Boesch, personal communication).

Other investigators have designed special MR sequences for the detection of eye movements (Jager *et al.,* 1997; Speeg-Schatz *et al.,* 1998) but have not reported their use during cognitive tasks. Furthermore, such methods do not allow the determination of actual eye position and thus would have limited usefulness for measuring the direction of gaze.



1053-8119/00 $35.00

Recently, Greenlee and colleagues have described an infrared fiber optic system for recording eye movements (Greenlee *et al.,* 1999). Although this method has very good resolution, its apparent limitation to recording horizontal eye position would again limit the determination of the absolute point of gaze.

In this report, we describe a long-range, infrared, video-oculographic system for recording eye movements in real time and in two dimensions while subjects performed attention tasks requiring either central fixation or saccades. The advantages of this technique include rapid calibration, accuracy, online feedback of the subject's performance, artifact-free eye movement traces, and no evidence of interference with the MR imaging signal.

## METHODS

### Subjects

Three healthy volunteers (two females and one male, 25–29 years of age) participated in the functional imaging portion of the study. All subjects were right handed by self-report and scored 90–100 on the modified Edinburgh handedness scale (Ransil and Schachter, 1994). A male subject (age 40) underwent scanning for the human noise dataset. High-speed eye data were collected on a female subject (age 24) as part of another protocol. All subjects gave their informed consent. This study was approved by the Institutional Review Board at Northwestern University.

### Behavior

The behavioral task was designed to induce shifts of spatial attention (Gitelman *et al.,* 1999; Posner, 1980). The display consisted of a small central diamond (1° wide) and two peripheral squares (1.5° wide and 7.5° eccentric in each visual field). During the active condition, one side of the central diamond formed an arrow which cued the side for subsequent target appearance. The cue stayed on during a cue-to-target interval of 200, 400, or 800 ms. A target ("X" or "+") then appeared for 100 ms on the same side as the cue 80% of the time (valid) or on the opposite side 20% of the time (invalid). Subjects were to respond only to an "X". Each trial lasted 2 s. During Covert runs, subjects discriminated the target while maintaining central fixation. During Overt runs subjects discriminated the target while looking at it, i.e., they saccaded to the target.

In the baseline condition for both the Covert and the Overt tasks, the central diamond and both side boxes were displayed every 2 s. The central diamond was either bold or not, and the side boxes contained either an "X" or a "+" on both sides. Subjects responded only if the central stimulus was bold, regardless of the shape of the peripheral targets. They maintained central fixation during the baseline condition for both Covert and Overt tasks. For both tasks, the numbers of total trials in each condition (120) were equivalent. There were 60 trials requiring responses in the active task and 56 in the baseline task. The fMRI experimental runs were designed as a series of paired active and baseline conditions each lasting 30 s and alternating a total of four times. Each task (Covert or Overt) was repeated twice. Therefore during each active or rest condition there was the opportunity to make approximately 240 saccades [15 trials per condition $\times$ 4 repeats $\times$ 2 runs $\times$ 2 saccades per cue (left or right saccade followed by a return to center for the next trial)].

### Eye Movements

Eye movements were monitored using the Applied Science Laboratories Model 504 eye tracking system (ASL, Waltham, MA) adapted to the MR environment. All modifications described below were supplied as part of ASL's commercial package. (1) The lens allowed focusing at distances of 2.74 to 4.88 m from the subject's eye. For the tests in this report, the system was located 2.98 m from the eye and 1.52 m from the rear opening of the magnet. (2) Power was supplied to the camera and light source using cables designed to run through a filtered connection. (3) The video signal from the camera was converted to an optical signal and transmitted out of the magnet room using a pair of fiber optic transmitter and receiver units (Polaris Industries, Atlanta, GA). The ASL control unit and a 486 PC running the ASL software were located in the MR control room 22.86 m from the eye–camera optical unit.

The accuracy of the ASL system is nominally less than 1° of visual angle using the described setup. However, performance may actually be better in the MR environment as subjects' head motion is quite restricted compared with the usual usage in the laboratory. In the current experiments, the minimum accuracy was 0.75° and the maximum was less than 0.5° (best case shown in Fig. 2).

The subject's eye was imaged via a mirror (4.8 $\times$ 3 cm) designed to allow (1) unobtrusive viewing of the eye by the camera and (2) an unimpeded view of the behavioral stimuli by the subject (Fig. 1). This mirror was a $\frac{3}{8}$-in. thick, $\frac{1}{4}$-wave-flat, BK7 glass window coated on the front surface with enhanced silver, which is highly reflective in the near infrared. Focusing the camera on the eye generally took less than 2 min. Positioning of the eye camera and mirror system was aided by illuminating the subject's eye with visible light filtered by a 10% transmission neutral density filter instead of the infrared filter.

Calibration of the subject's point-of-gaze took approximately 5 min. using the 9-point calibration routine

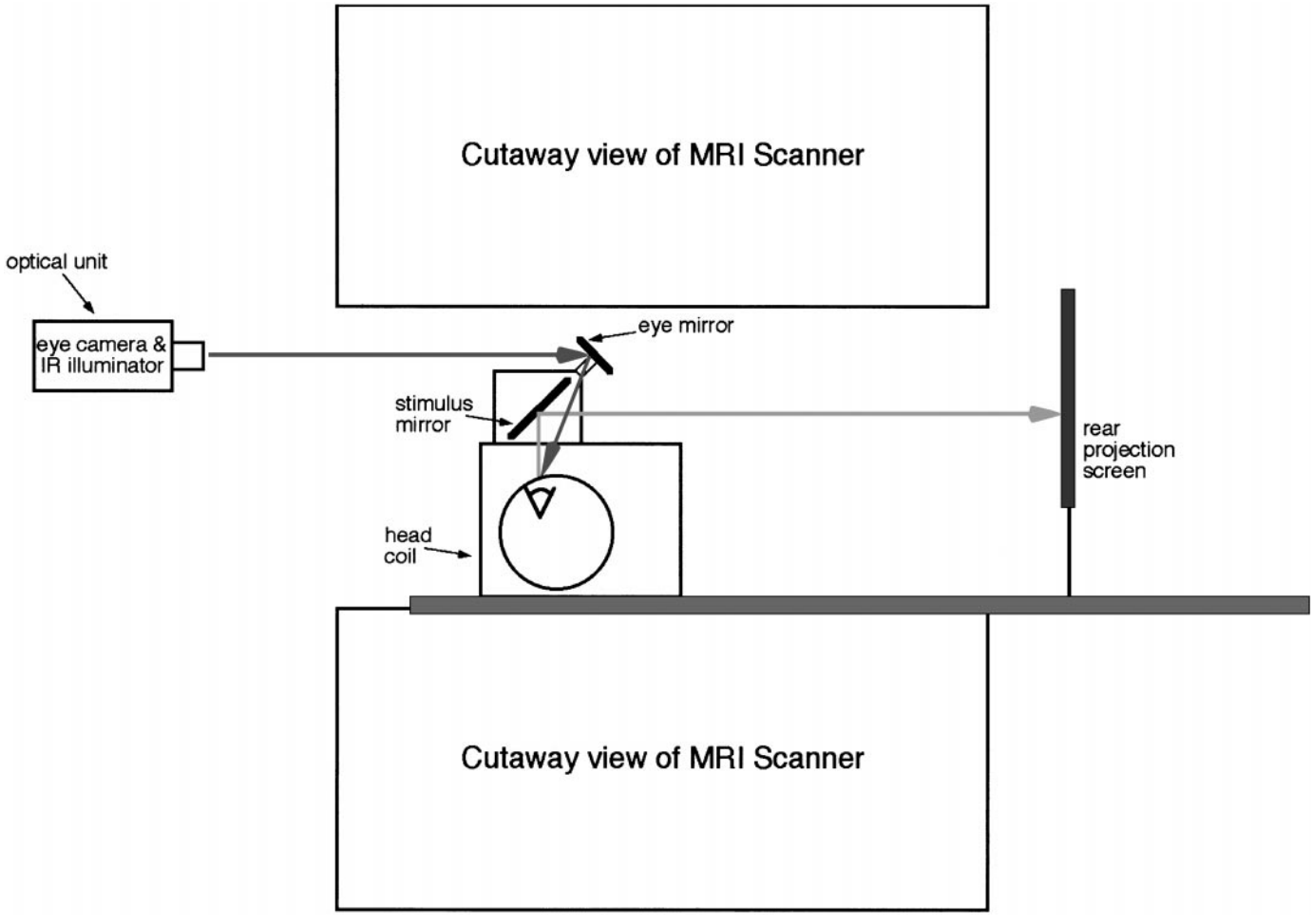


**FIG. 1.** Schematic of the mirror system on the head coil illustrating the light paths for both the optical unit and the subject. The positions of the mirrors allow unobstructed views for both the eye camera and the subject. During imaging, the subject can see only a minimal dull red glow of the infrared light source if he or she looks directly into the eye mirror.

built into the ASL software. The calibration did not drift throughout a 60-min imaging session. Eye position was sampled at a rate of 60 Hz. An additional subject also underwent eye-movement monitoring at 120 Hz to demonstrate the feasibility of recording at this higher acquisition speed. Time locking of the eye data and stimulus presentation can be accomplished in two ways: (1) operator-generated flags can mark the occurrence of various stimuli or (2) 16-bit TTL data can be sent from the stimulus presentation computer, similarly marking stimulus events. Both methods were used in the current report.

### MR Imaging

The MR acquisition and the fMRI analysis techniques have been previously described (Gitelman *et al.*, 1999). Functional images were acquired on a 1.5-T Siemens Vision system using single-shot echo planar imaging (TR/TE 4350/40 ms, 32 transaxial slices, voxel size 3.75 × 3.75 × 4 mm). Sixty volumes were acquired per run and the 4 initial volumes were discarded to allow for signal stabilization. Subjects' heads were immobilized with a vacuum pillow (Vac-Fix; Bionix, Toledo, OH) and the restraint calipers built into the head coil. Responses were recorded using a nonmagnetic button. T1-weighted anatomic images used a 3D FLASH sequence (TR/TE 15 ms/6 ms, flip angle 20°, voxel size 0.94 × 0.94 × 1 mm).

For the noise analysis a water phantom was scanned using identical parameters. One hundred twenty-eight volumes were acquired under three conditions (power on/front cover removed, power on/front cover in place, and no equipment). Since the optical unit is easier to focus with the front cover removed, the influence of its removal on the amount of noise was specifically tested. Scanning was repeated three times for each phantom

condition. A human subject was similarly scanned during rest with no equipment in the room for comparison with the phantom.

### Eye-Movement Analysis

Eye-movement data were analyzed and displayed using custom-designed software (ILAB 2.76; Cognitive Neurology and Alzheimer's Disease Center and Darren Gitelman) written in Matlab (Mathworks, Sherborn, MA). The eye-movement data were filtered to remove blink artifacts.

### Noise Analysis

The phantom and human rest MRI data were motion corrected. A region of interest (ROI) measuring $16 \times 16$ voxels was selected from the middle portion of the central slice of the phantom. In the human data, a smaller region of interest (42 voxels) was chosen from the parietal white matter. The human ROI was selected to avoid blood vessels, cerebrospinal fluid, and heterogeneous tissue in order to obtain a minimum noise estimate in the brain for comparison with the phantom.

The ROIs from the phantom and human rest data were subjected to power spectral analysis (Zarahn *et al.,* 1997). The power spectral data were normalized to the DC component for each series to allow direct comparisons. The stability of the MR signal was tested in all three phantom conditions and in the human data by calculating the signal change from baseline as a percentage of the mean signal over time. The average deviation for each condition is reported.

### fMRI Analysis

Analysis of subjects' fMRI data was performed using SPM96 software (Wellcome Department of Cognitive Neurology, London, UK) running in Matlab (Friston *et al.,* 1995; Worsley and Friston, 1995) on a HP-UX (Hewlett–Packard, Palo Alto, CA) workstation. The functional MRI data were motion corrected, normalized into standard anatomical space, and smoothed (7-mm isotropic kernel). Contrasts were set up to test for voxel-wise effects of signal differences between the baseline and the active conditions, and SPM$|Z|$ maps were calculated (Friston *et al.,* 1995). Data from the three subjects were reviewed individually and combined in a fixed-effects group analysis. The group

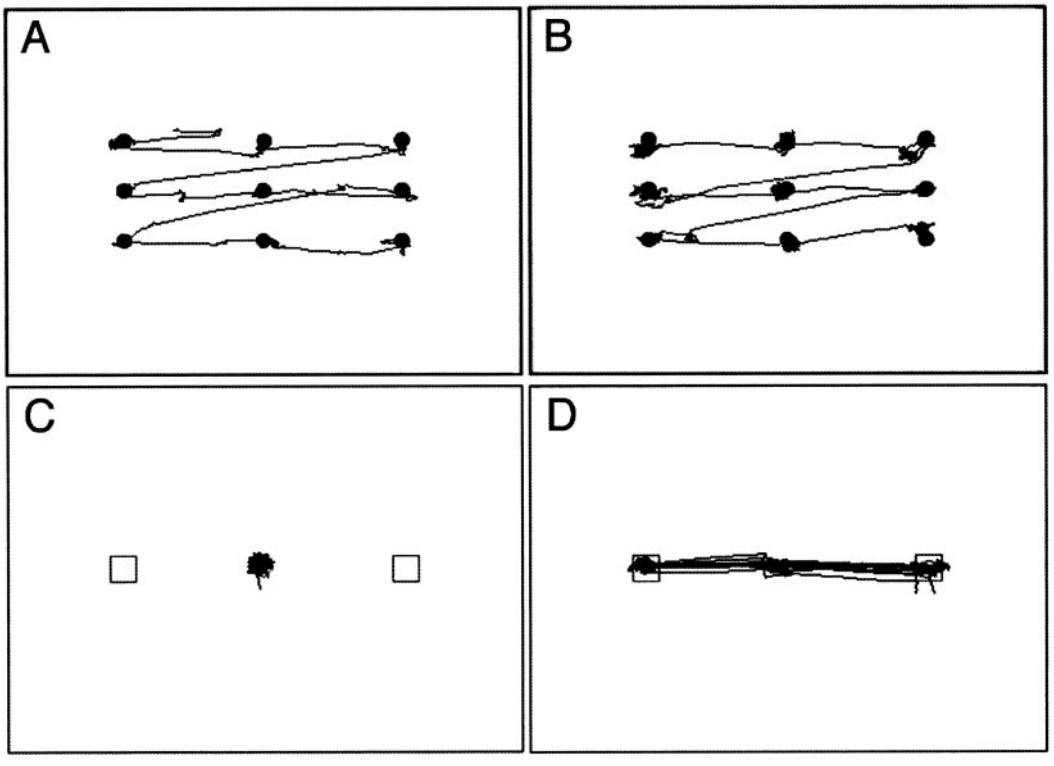


**FIG. 2.** Eye-movement plots for subject 1 (A, C, and D). (A) Calibration plot demonstrating close correspondence between the targets and the subject's eye movements. The calibration targets are separated by 2.8° vertically and 7.3° horizontally. (B) Calibration plot performed at 120 Hz in a different subject. (C) Plot of eye movements during the active condition of the Covert task for one 30-s period. Excellent central fixation by the subject can be seen. (D) Plot of eye movements during the active condition of the Overt task for one 30-s period. Accurate saccades to the target boxes are illustrated.

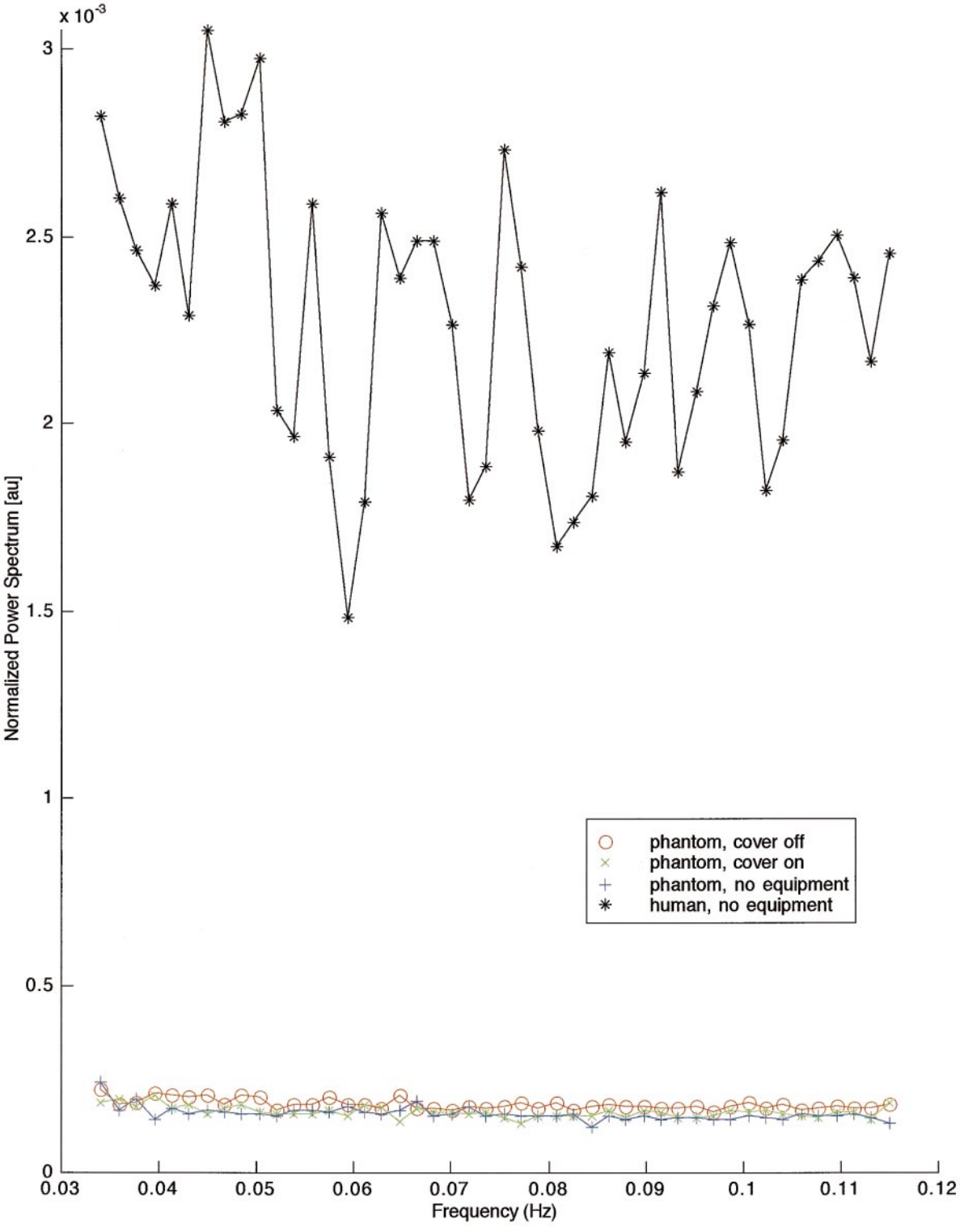


**FIG. 3.** Normalized power spectrum plot for the phantom and human data. Although a significant difference was seen between the power spectra of the power on/cover off condition and the other two phantom scanning conditions (power on/cover on and no equipment), these differences are far less than those between the phantom and the human spectra. Note that frequencies below 0.03 Hz are not shown, as there was typical increasing power at these lower frequencies which would have distorted the graph (Zarahn *et al.,* 1997). No additional differences were seen at the lower frequencies.

**TABLE 1**

Percentage Signal Variation in Each Condition

| Condition | Percentage signal variation (mean ± SD) |
|---|---|
| Phantom—power on/cover off | 0.366 ± .036%* |
| Phantom—power on/cover on | 0.346 ± .034% |
| Phantom—no equipment | 0.340 ± .037% |
| Human—rest | 1.570 ± .290% |

* $P < 0.05$ for the power on/cover off condition versus the power on/cover on or no equipment phantom conditions.

statistical parametric maps were thresholded at $P < 0.05$ corrected for the whole brain volume and overlaid on the subjects' averaged T1 image.

## RESULTS

### Behavior

All subjects tolerated the procedure well and reported no discomfort. In the Covert active condition subjects were 86.7% accurate and showed reaction times of 472 ± 90 ms (mean ± SD), for valid trials, and 552 ± 134 ms for the invalid trials ($P < 0.05$). In the Overt active condition subjects were 75% accurate and showed reaction times of 444 ± 46 ms for valid trials and 624 ± 85 ms for invalid trials ($P < 0.05$). During the baseline condition subjects were 99% accurate and reaction times were 339 ± 47 and 324 ± 20 ms for the Covert and Overt tasks, respectively ($P > 0.05$ comparing the baselines).

### Eye Movements

The eye-movement calibration data for one subject overlaid on the calibration point positions are shown in Fig. 2A. Excellent correspondence is seen between the point of gaze and the calibration points. Figure 2B shows similar accuracy at the 120-Hz acquisition speed in another subject. Figure 2C demonstrates the eye movements during one 30-s period of the Covert task, showing maintenance of fixation by the subject. The eye movement data during a 30-s period of the Overt task are shown in Fig. 2D. There was no evidence of any artifacts in the eye movement data induced by the MR acquisition.

During the Covert task, subjects made 3.0 ± 1.0 saccades during 8 min of scanning in the baseline condition and 1.3 ± 1.2 saccades during the same amount of time in the active condition ($P > 0.1$). In the Overt task, baseline performance was 7.3 ± 4.0 saccades in 8 min versus 213 ± 15.1 saccades during the active condition ($P < 0.002$). There was no significant difference in the baseline condition saccades between the Covert and the Overt tasks ($P > 0.1$).

### Phantom Noise Analysis

A plot of the normalized power spectra for the phantom and human data is shown in Fig. 3. A significant difference was seen between the power on/cover off

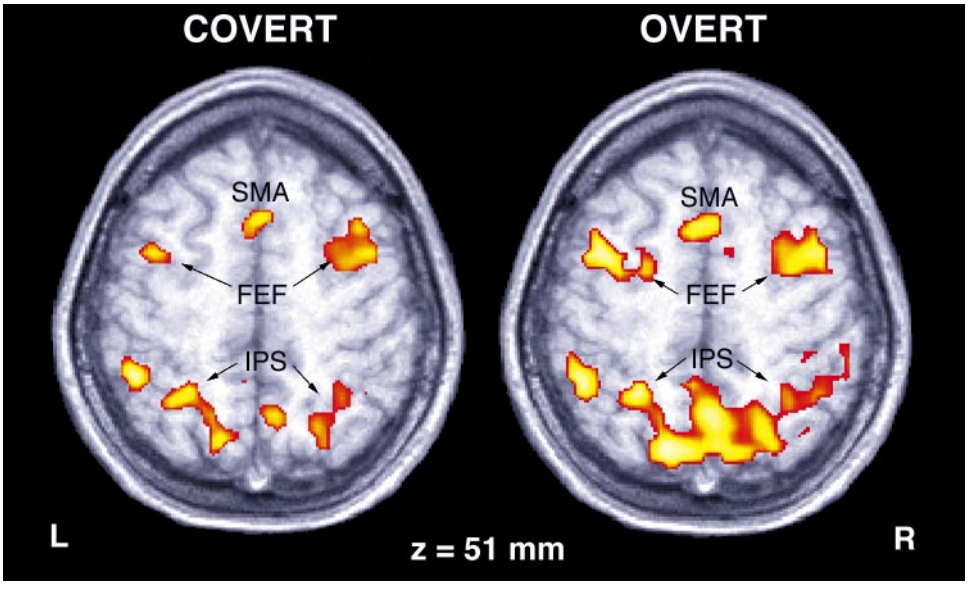


**FIG. 4.** Representative activations in the Covert and Overt tasks at the level of the frontal eye fields for all subjects. Right is on the right side of the images, as indicated. FEF, frontal eye fields; IPS, intraparietal sulcus; SMA, supplementary motor area.

and the other two scanning conditions: power on/cover on ($t_{88} = 6.6$, $P < 0.001$) and no equipment ($t_{88} = 7.1$, $P < 0.001$). However, there was no significant difference between the power on/cover on and no equipment conditions ($t_{88} = 1.1$, $P > 0.1$). The signal variance showed similar differences between conditions. Figure 3 also demonstrates that any differences among the three phantom conditions were far less than the signal changes seen in human resting data (see Table 1).

### MRI Data

In both Covert and Overt tasks clear activations were seen involving the frontal eye fields (FEF), intraparietal sulci, and supplementary motor cortex. The FEF activation in the Covert task was centered at left, −36, 3, 54, and right, 30, −3, 45. In the Overt task the FEF location was left, −36, 3, 54, and right, 33, −3, 48. These areas are consistent with previous reports examining activations in both overt and covert spatial attention tasks and saccadic eye movements (Corbetta *et al.,* 1993; Gitelman *et al.,* 1999; Kim *et al.,* 1999; Nobre *et al.,* 1997; Paus, 1996; Petit *et al.,* 1993). Other areas of activation not shown in Fig. 4 included right more than left prefrontal cortex and insula, right cingulate gyrus, temporo-occipital cortex bilaterally, and basal ganglia. The Overt task also had activations in primary and association visual cortices and in the cerebellum bilaterally.

## CONCLUSIONS

We report a method for the accurate and sensitive real-time monitoring of eye movements during fMRI. Analyses of the power spectra and signal variance from a phantom scanned under different conditions demonstrated no significant effect of the eye-movement equipment on the MR signal, particularly when the optical unit's front cover was in place. However, even with the optical unit open, the amount of signal change was still far less than that seen in human resting data, suggesting negligible noise from the eye-movement equipment under standard operating conditions.

Using this system we found that a task based on covert shifts of spatial attention led to FEF activation despite the subjects' ability to maintain central fixation. Although some surreptitious saccades did occur during the active task they were not significantly more prominent than those during the baseline condition. These results provide the most reliable demonstration to date, in the population studied, that the FEF activation in tasks of covert spatial attentional shifts can be attributed to the attentional contingency rather than surreptitious eye movements. We also found a nearly identical FEF activation in a task of overt shifts of spatial attention, providing further support for the contention that the FEF provides an area of overlap for the neural networks subserving spatial attention and oculomotor control (Corbetta, 1998; Gitelman *et al.,* 1998; Nobre *et al.,* 1998).

## ACKNOWLEDGMENTS

This work was supported by the McDonnell–Pew Program in Cognitive Neuroscience (D.R.G.), by NIH Grant NS30863-04 (M.M.M.), and by a NARSAD young investigator award (K.S.L.). We are grateful to Roger Ray for assistance with programming, to Oliver Josephs of the Wellcome Department of Cognitive Neurology (London, UK) and Josh Borah of ASL for critical technical assistance, and to Richard Niemczura and Terry Cunningham for assistance with image acquisition.

## REFERENCES

Brandt, S. A., Reppas, J., Dale, A., Wenzel, R., Savoy, R., and Tootell, R. 1997. Simultaneous infra-red oculography and fMRI. *Proc. Int. Soc. Magn. Reson. Med.* **3:**1978. [Abstract]

Corbetta, M. 1998. Frontoparietal cortical networks for directing attention and the eye to visual locations: Identical, independent, or overlapping neural systems? *Proc. Natl. Acad. Sci. USA* **95:**831–838.

Corbetta, M., Miezin, F. M., Shulman, G. L., and Petersen, S. E. 1993. A PET study of visuospatial attention. *J. Neurosci.* **13:**1202–1226.

Culham, J. C., Brandt, S. A., Cavanagh, P., Kanwisher, N. G., Dale, A. M., and Tootell, R. B. H. 1998. Cortical fMRI activation produced by attentive tracking of moving targets. *J. Neurophysiol.* **80.**

Felblinger, J., Müri, R. M., Ozdoba, C., Schroth, G., Hess, C. W., and Boesch, C. 1996. Recordings of eye movements for stimulus control during fMRI by means of electro-oculographic methods. *Magn. Reson. Med.* **36:**410–414.

Friston, K. J., Holmes, A. P., Worsley, K. J., Poline, J.-B., Frith, C. D., and Frackowiak, R. S. J. 1995. Statistical parametric maps in functional imaging: A general linear approach. *Hum. Brain Mapp.* **2:**189–210.

Gitelman, D. R., Nobre, A. C., Kim, Y. H., Parrish, T. B., LaBar, K. S., and Mesulam, M.-M. 1998. Activation of overlapping but not identical frontal and parietal regions by saccadic eye movement and overt spatial attention tasks. *NeuroImage* **7:**68.

Gitelman, D. R., Nobre, A. C., Parrish, T., LaBar, K. S., Kim, Y.-H., Meyer, J. R., and Mesulam, M. M. 1999. A large-scale distributed network for covert spatial attention: Further anatomical delineation based on stringent behavioral and cognitive controls. *Brain* **122:**1093–1106.

Greenlee, M. W., Kimmig, H., Huethe, F., Gondan, M., and Mergner, T. 1999. MR-EYETRACKER: A new method for measuring eye movements in functional MRI. *NeuroImage* **9:**S249.

Jager, L., Welge-Lussen, U., Lanzl, I., and Reiser, M. 1997. Imaging of eye movement with fast MRI. *J. Comput. Assisted Tomogr.* **21:**447–451.

Kim, Y.-K., Gitelman, D. R., Nobre, A. C., Parrish, T. B., LaBar, K. S., and Mesulam, M.-M. 1999. The large scale neural network for spatial attention displays multi-functional overlap but differential asymmetry. *NeuroImage* **9:**269–277.

Nobre, A. C., Dias, E. C., Gitelman, D. R., and Mesulam, M. M. 1998. The overlap of brain regions that control saccades and covert visual spatial attention revealed by fMRI. *NeuroImage* **7:**S9.

Nobre, A. C., Sebestyen, G. N., Gitelman, D. R., Mesulam, M. M., Frackowiak, R. S. J., and Frith, C. D. 1997. Functional localisation of the neural network for visual spatial attention by positron-emission tomography. *Brain* **120:**515–533.

Paus, T. 1996. Location and function of the human frontal eye-field: A selective review. *Neuropsychologia* **34:**475–483.

Petit, L., Orssaud, C., Tzourio, N., Salamon, G., Mazoyer, B., and Berthoz, A. 1993. PET study of voluntary saccadic eye movements in humans: Basal ganglia–thalamocortical system and cingulate cortex involvement. *J. Neurophysiol.* **69:**1009–1017.

Posner, M. I. 1980. Orienting of attention. *Q. J. Exp. Psychol.* **32:**3–25.

Ransil, B. J., and Schachter, S. C. 1994. Test–retest reliability of the Edinburgh handedness inventory and global handedness preference measurements, and their correlation. *Percept. Mot. Skills* **79:**1355–1372.

Speeg-Schatz, C., Scheiber, C., Passard, C., and Grucker, D. 1998. Video loop MRI of ocular motility: A new technique: Turbo rare sequence at 2 T for the study of horizontal gaze. *Binocular Vision Strabismus Q.* **13:**105–114.

Worsley, K. J., and Friston, K. J. 1995. Analysis of fMRI time-series revisited—Again. *NeuroImage* **2:**173–181.

Zarahn, E., Aguirre, G. K., and D'Esposito, M. 1997. Empirical analyses of BOLD fMRI statistics. *NeuroImage* **5:**179–197.